

Can functional group composition of alkaline isolates from black carbon-rich soils be identified on a sub-100 nm scale?



Karen Heymann^a, Johannes Lehmann^{a,*}, Dawit Solomon^a, Biqing Liang^a, Eduardo Neves^b, Sue Wirick^c

^a Department of Crop and Soil Sciences, Cornell University, Ithaca, NY, USA

^b Museu de Arqueologia e Etnologia, Universidade de Sao Paulo, Sao Paulo, SP 05508-900, Brazil

^c Department of Physics and Astronomy, State University of New York at Stony Brook, Stony Brook, NY, USA

ARTICLE INFO

Article history:

Received 6 December 2013

Received in revised form 9 July 2014

Accepted 10 July 2014

Available online xxxx

Keywords:

Alkaline extracts

Pyrogenic carbon

Soil organic matter

Humic substances extracts

STXM–NEXAFS

ABSTRACT

Objectives: Alkaline extracts from soils generate operationally-defined isolates that are referred to as “humic substances” but may not relate to a distinct molecular structure within the soil organic matter (SOM) matrix. This study examines whether alkaline extracts from black carbon (BC) rich soils can be identified on a fine spatial scale.

Methods: We related the functional group composition of alkaline extracts derived from BC-rich soils using Scanning Transmission X-ray Microscopy (STXM) coupled with near-edge X-ray absorption fine-structure (NEXAFS) spectroscopy to the spatial composition of a BC-rich soil microaggregate at a scale of <50 μm. Soils were analyzed from 3 depths (0–0.16 m, 0.16–0.43 m, 0.43–0.67 m) along with their respective extracts.

Results: Using principal component analysis, we were unable to obtain a good fit (RMS < 0.01) for the spectral properties of the alkaline extracts within the spatial map of the microaggregates. The presence of a distinct chemical structure resembling the alkaline extracts could not be verified within the soil organic matter matrix on a fine spatial scale.

Conclusions: Our results suggest that a distinct component class similar to alkaline extracted materials, often referred to as “black humic substances”, is not present in SOM on a fine spatial scale. Rather, alkaline extracts of BC-rich soils reflect the mixture of various materials at different stages of decomposition.

© 2014 Elsevier B.V. All rights reserved.

1. Introduction

The severe climatic consequences of potentially large organic C losses from rapidly warming terrestrial ecosystems (Schuur et al., 2013) highlight the importance of understanding the underlying biogeochemical processes essential to building accurate global C and climate models. Relatively little is known about the complex mechanisms controlling organic C turnover in terrestrial systems (Kleber, 2010; Schmidt et al., 2011).

The chemical composition and spatial association of soil organic matter (SOM) has been the subject of much debate for well over a century, and particularly the importance of isolates using alkaline extraction (Burdon, 2001; Kleber and Johnson, 2010; Sutton and Sposito, 2005). Many studies of SOM characterization have historically utilized alkaline extracts, which are described as isolating complex, heterogeneous compounds formed during the decay and transformation of plant and microbial remains, and are often referred to as a compound class called humic substances (Schulten and Schnitzer, 1993; Sutton and Sposito, 2005). However, contemporary analyses of soil organic

matter have suggested that SOM may consist of spatially highly complex mixtures of simple biomolecules (Kelleher and Simpson, 2006; Lehmann et al., 2008) rather than traditionally defined humic substances isolated by alkaline extraction.

Lack of direct observational evidence of the presence of the functional group composition identified in alkaline extracts within the soil matrix (Lehmann et al., 2008) also brings into question references to a distinct class of compounds said to form from black carbon (BC) and extracted using the same alkaline extraction procedure, often called “black humic substances”. BC is the product of incomplete combustion of plant biomass and fossil fuels, and can in some locations comprise a fairly substantial portion of SOM (Hedges et al., 2000). Compounds isolated from BC-rich soils using alkaline extraction have been suggested to play an important role in degradation processes in soil (Ascough et al., 2011; Hiradate et al., 2004; Kumada, 1983; Nishimura et al., 2006; Shindo et al., 1986a,b,c, 2004, 2005). Mineralization of BC to carbon dioxide has indeed been described in many studies (e.g., Baldock and Smernik, 2002; Cheng et al., 2008). However, it is not clear whether organic compounds remaining from decomposition of BC are fundamentally different than those of uncharred organic matter (Hockaday et al., 2006) and whether these are captured in alkaline extracts. While the contribution of BC to alkaline extracts of SOM has been recognized (Masiello and Druffel, 1998), the question remains whether compounds isolated with

* Corresponding author.

E-mail address: CL273@cornell.edu (J. Lehmann).

alkaline extractions can actually be identified on a fine spatial scale in soil.

The main objective of our study was therefore to characterize alkaline extracts derived from a soil rich in BC. Further, our objective was to compare the functional group composition of these alkaline extracts with that of SOM observed directly at a fine spatial scale.

2. Methods

2.1. Study site

Black C-rich Anthrosols were obtained from an archeological site, Lago Grande (LG), near Manaus, Brazil (3°8' S, 59°52' W, 40–50 m above sea level). Details concerning soil formation conditions and local climate and vegetation have been described elsewhere (Liang et al., 2006). A depth profile of the soil from 0–0.67 m was obtained from horizons at 0–0.16 m, 0.16–0.43 m, and 0.43–0.67 m (Table 1) (Liang et al., 2013), in order to examine a gradient of organic matter whose functional group composition in alkaline extracts is typically found to systematically vary with depth (Kögel-Knabner et al., 1991).

Microaggregates were isolated from all three horizons as described by Kinyangi et al. (2006). Free stable aggregates with a size between 20 and 200 μm were prepared for spectroscopic measurement from each soil as follows: aggregates were misted, shock-frozen and sectioned using a cryo-microtome (Ultracut UTC, Leica Microsystems Inc., Bannockburn, IL), sections were cut at $-55\text{ }^\circ\text{C}$ to a thickness of 100–200 nm using a diamond knife (MS9859 Ultra 458, Diatome Ltd., Biel, Switzerland) at a cutting speed of 0.3 to 1.2 mm s^{-1} (angle of 6°) and transferred to Cu grids (carbon free, 200 mesh, silicon monoxide No. 53002, Ladd Research, Williston, VT) which were impregnated with silicon monoxide (SiO) substrate. Each grid was mounted onto the center pinhole of stainless steel sample stage plates (diameter of 46 mm).

Soil alkaline extracts were obtained using the methods recommended by the International Humic Substances Society (IHSS) (Swift, 1996). Soils were extracted with 0.5 M NaOH at a soil:solution ratio of 1:10 (mass:volume) under N_2 atmosphere (Stevenson, 1994). These extracts were further separated into alkaline but acid-insoluble extracts, often referred to as yielding “humic acid extracts”, and alkaline but acid-soluble extracts, often referred to as generating “fulvic acid extracts”, by acidifying the extract to pH 2 using 6 M HCl and precipitating acid-insoluble organic matter to be removed from acid-soluble organic matter.

2.2. STXM and C 1s NEXAFS data acquisition

Spectroscopic measurements were performed at beamline X1A1 of the National Synchrotron Light Source, Brookhaven National Laboratory which is equipped with a Scanning Transmission X-ray Microscopy (STXM) endstation. The STXM beamline consists of a tunable undulator inserted into the electron storage ring (2.8 GeV; generating a high flux of spatially coherent photons per second in the soft X-ray region), a spherical grating monochromator (tunable over 250–800 eV), and an endstation containing a steeper and piezo stage and a 160- μm Fresnel zone plate (45 nm spatial resolution) used as the focusing optic. The monochromator was calibrated using CO_2 to the adsorption band at 290.74 eV before each session (Sham et al., 1989).

Table 1
Profile characteristics of the studied Amazonian Dark Earth soil (Liang et al., 2013).

Depth (m)	Sand (%)	Silt	Clay	Total C (mg g^{-1})	BC (mg g^{-1})	BC (% of C)	CEC ($\text{mmol}_\text{C} \text{kg}^{-1}$)
0–0.16	46.7	28.0	25.3	29.0	18.0	62.2	292
0.16–0.43	43.4	26.0	30.5	21.3	16.4	77.0	264
0.43–0.67	44.3	25.3	30.4	19.1	14.6	76.2	258

To determine functional group composition of the alkaline extracts, extracts were mounted on 100-nm thick Si_3Ni_4 windows (Silson Ltd., Northampton, UK) by dissolving 1 mg of sample in 400 μL of pure trifluoroacetic acid (TFA, Sigma-Aldrich Corp., St. Louis, MO), transferring 1 μL of solution onto the window (Boese et al., 1997; Solomon et al., 2009) and drying them at $35\text{ }^\circ\text{C}$. Single point spectra were collected in triplicate, where the grating is moved from 280 to 310 eV with 0.1 eV energy step, and 120 ms dwell time. After high-resolution micro-graphs of the samples were taken using the STXM (see information above) to locate the area of uniform thickness of the sample film, the illuminated spot on the samples was then increased to 10 μm by defocusing the zone plate to avoid beam damage through decreasing the required signal over a large area (Boese et al., 1997; Solomon et al., 2007, 2009). Sequential measurements indicated no detectable beam damage. Background spectra (I_0) were collected from a sample-free region of each Si_3Ni_4 window. Samples were measured under He atmosphere. The three spectra per sample were then confirmed to be in agreement with each other and averaged. WinXas 3.1 (WinXAS Software, Hamburg, Germany) was used to baseline correct and normalize the data.

To map the microaggregates, the z-stage was adjusted to focus the X-rays through the microaggregate sample section. Beamline-slit openings for a horizontal slit upstream of the monochromator; a vertical slit downstream of the monochromator; and the exit slit were set at 40/25/25 μm to give an energy resolution of 0.1 eV (Winn et al., 2000). The slit settings and zone plate together provided a scanning spatial resolution of approximately 50 nm. Two step sizes were used: 500 nm for an overview of a microaggregate and 50 nm for detailed observations (Lehmann et al., 2008). The monochromator energy was increased from 280 to 282.5 eV in 0.3 eV increments (scan time: 1 ms), from 282.5 to 292 eV in 0.1 eV steps (scan time: 3 ms), and from 292 to 310 eV in 0.3 eV steps (scan time: 3 ms). Smaller energy steps of 0.1 eV were chosen in the main spectroscopic regions where C 1s core electron excitation is indicative of sharp 1s 2p*, and broad 1s, 3p 1s* transitions. Dwell times were increased in energy regions of specific interest. Some beam damage cannot be completely avoided, but previous research using NEXAFS at the same STXM beamline has shown that beam damage at the studied dwell times was not significantly changing spectral properties (Ade et al., 1992) and effective exposure is much lower than in point spectra (Ade and Hitchcock, 2008). The calculated photon dose on the samples ranged between 10^5 and 10^7 Gy, significantly below the doses of 10^9 Gy conservatively estimated to result in beam damage of less than 20% (Schäfer et al., 2009) under identical operating conditions than in this study. Single images were recorded at each photon energy level and built into a stack using the program Stack Analyze 2.6.1 (Jacobsen et al., 2000). Alignment was performed using cross-correlation. Stack image processing software and data analyses instructional manuals can be accessed on the website at <http://xray1.physics.sunysb.edu/data/software.php>.

Black C particles were manually picked from the soil using super tweezers (N5, Dumont, Montignez, Switzerland) under a light microscope (303; SMZ-10, Nikon, Japan). Plant litter was manually harvested from the O horizon of soil. A microbial extract (ME) was obtained from the soil as follows: bacteria [gram (–) *alphaproteobacteria*] colonies were extracted from the soil, cultivated in broth (Bacto peptone 10 g, yeast extract 5 g, NaCl 5 g L^{-1}) and distributed into 5 mL aliquots in screw top tubes and sterilized for 15 min at $121\text{ }^\circ\text{C}$. An aliquot (1 mL) of the sterilized bacterial culture (after 24 h, $37\text{ }^\circ\text{C}$) was transferred to Eppendorf tubes and centrifuged at 5000 rpm for 5 min, and sequentially washed (2 \times) with 0.05 M NaCl after discarding the supernatant. Samples were dried and stored under desiccant until measured (Liang et al., 2008).

2.3. Data analysis

For NEXAFS data, peak resonances with specific bonding environments were assigned based on the spectral signatures of pure chemical

Table 2

Proportion (%) of functional group distribution of alkaline extracts insoluble or soluble in acid obtained using deconvolution of C NEXAFS spectra (spectra shown in Fig. 1).

	Depth (m)	Aromatic (G1 + G2 + G3)	Phenolic (G4)	Alkyl (G5)	Carboxylic (G6)	O-alkyl (G7 + G8)
Insoluble	0–0.16	29	11	5	29	26
Insoluble	0.16–0.43	33	8	9	18	32
Insoluble	0.43–0.67	37	7	1	22	33
Soluble	0–0.16	25	13	4	30	28
Soluble	0.16–0.43	42	7	5	18	28
Soluble	0.43–0.67	35	10	5	32	18

standards representative of specific functional groups (Solomon et al., 2009), and a least-squares fitting scheme was applied to the normalized NEXAFS spectra in the range of 280 to 310 eV. We used a scheme based on eight Gaussians curves (labeled “G1”, etc.) following the procedure suggested by Scheinost et al. (2001), with additional bands for substituted aryl C (G3) (Lehmann et al., 2005; Liang et al., 2008) and an additional carbonyl group (G8) (Heymann et al., 2011). Average positions for the Gaussian bands of environmental BC have been identified previously (Heymann et al., 2011), and were assigned to 284.5 eV for aromatic or quinone C=O (G1); 285.4 eV for aromatic C=C (G2); 286.1 eV for aromatic C=O (G3; Lehmann et al., 2005); 286.7 eV for aromatic C=C–OH indicative of lignin type C (G4); 287.6 eV for alkyl C (G5); 288.4 eV for carboxyl C and amide C–N (G6); 289.2 eV for O-alkyl C (G7); and 289.9 eV for O-alkyl C (G8). It should be noted that C species overlap in the NEXAFS region and the Gaussian curves typically capture a range of bonds (Lehmann et al., 2009). An arctangent function was used to model the ionization step and was fixed at 290 eV. The full width at half maximum of the bands was set at 0.4 ± 0.2 eV, while the amplitude was floated during the fit. Deconvolution was performed by resolving spectra into individual arctangent and Gaussian curve components using the ATHENA software (ATHENA 0.8.052; Ravel and Newville, 2005). Spectral regions represented by Gaussian curves were described as being generally attributed to the following functional groups: overall aromatic type C was represented by the sum of the [G1 + G2 + G3] peaks (Table 2); aromatic C with side chain substituent (such as phenolic C) by the G4 peak; alkyl C by the G5 peak; carboxylic/carbonyl C by the G6 peak; and O-alkyl C by the sum of [G7 + G8] peaks (Heymann et al., 2011; Lehmann et al., 2009).

For the maps obtained using STXM, the program PCA_GUI 1.1.1 was used to orthogonalize and noise-filter data, as well as to identify the

number of significant components ($s = 1, 2, 3, \dots, 10$) in the microaggregate as well as to group spectrally distinct pixels into clusters. Different numbers of components and clusters were used to identify the combination of components and clusters which yielded the lowest errors (acceptable below $RMS < 0.01$). Singular value decomposition (SVD) was calculated to obtain target maps and associated target spectra (Lehmann et al., 2005). Target spectra were used from the NEXAFS analyses of the two different alkaline extracts to identify whether they would explain a significant portion of a region in the maps, similar to the method used for total alkaline extracts of soils with low BC contents (Lehmann et al., 2008).

3. Results

3.1. Characterization of components

NEXAFS spectral properties of the two types of alkaline extracts (acid-soluble or acid-insoluble) appeared highly similar to one another (Fig. 1). The main peak positions were not systematically different between acid-insoluble and acid-soluble alkaline extracts, appearing at 285.0, 286.1 and 288.4 eV. The well resolved absorption band near 285 eV corresponds to the C $1s-\pi^*_{C=C}$ transition related to the protonated and alkylated to carbonyl substituted aryl-C (C=C) (Cody et al., 1998). A second well-resolved, less intense absorption band was present between 286.2 eV (mainly in the topsoil) and 286.5 eV (mainly in the subsoil) for both types of extracts, representing a mixture of unsaturated C at 286.1 eV (Lehmann et al., 2005) and phenolic type C at 286.7 eV. A third absorption band present around 288.4 to 288.7 eV for all extracts was very clearly resolved and indicates the presence of amide C–N to carboxyl/carbonyl type C (Liang et al., 2006).

We used spectral deconvolution results to compare the functional group distribution for the extracts (Table 2). The proportion of total C present in the aromatic C region (G1–G3) of the acid-insoluble alkaline extracts increased with depth, from 29% at 0–0.16 m depth to 37% at 0.43–0.67 m depth (Table 2). The phenolic and aliphatic type C regions (G4 and G5) did not exhibit distinct differences between the acid-insoluble alkaline extracts over the depth profile. The carboxylic/carbonyl/amide type C absorption region (G6) showed that at a depth of 0–0.16 m and 0.43–0.67 m the proportion of total absorption intensity present in this region was highly similar (22–29%) but was lower at a depth of 0.16–0.43 m (18%). The proportion of the O-alkyl type C region (G7 + G8) increased with depth, from 26% at a depth of 0–0.16 m to 33%

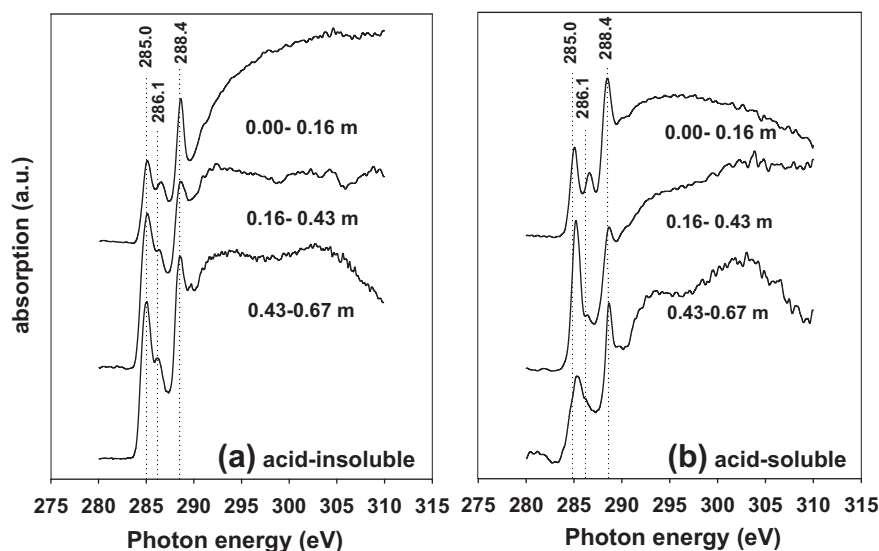


Fig. 1. Carbon 1s NEXAFS spectra of alkaline extracts (a) insoluble in acid and (b) soluble in acid from an Amazonian Dark Earth.

Table 3

Proportion (%) of functional group distribution of plant litter, microbial extracts and BC particles obtained using deconvolution of C NEXAFS spectra (spectra shown in Supplementary online material).

	Aromatic (G1 + G2 + G3)	Phenolic (G4)	Alkyl (G5)	Carboxylic (G6)	O-alkyl (G7 + G8)
Plant litter	15	13	13	25	34
Microbial extract	10	7	20	31	32
BC particles	41	11	13	19	16

at 0.43–0.67 m. The spectra of the acid-soluble alkaline extracts did not show consistent trends with depth.

Black C particles were characterized by a broad C 1s- $\pi^*_{C=C}$ transition at 285 eV (41% aromaticity) (Table 3), and a smaller C 1s- $\pi^*_{C=O}$ transition representing carboxylic-type C at 288.7 eV (19% of total absorption intensity). In contrast, the microbial extract was characterized by only a small peak around 285.3 eV (10% aromaticity) (Table 3). The proportions of total signal intensity in the aliphatic (20%), the carboxylic (31%) and the O-alkyl C (32%) region defined the material and distinguished it from the BC particles (Table 3). Plant litter was fairly heterogeneous with multiple peaks present near 284.5, 285, 288 and 289 eV. The aromatic, phenolic and aliphatic type C regions each comprised 13–15% of total absorption intensity. The proportion of C present in the carboxylic type C transition was around 25%, and the O-alkyl region value was around 34%.

3.2. Principal component and cluster analysis

Cluster analysis and principal component analyses were performed by systematically testing combinations of components and clusters for each sample (Figs. 2–5). This was done in order to determine whether the spatial distribution of the clusters was significantly affected by changing the number of principal components and to determine which combination would be the most representative of the sample.

For a depth of 0–0.16 m we mapped both an overview of the entire microaggregate with a step size of 500 nm (Fig. 2) as well as a close-up area of interest within the microaggregate with a step size of 50 nm (Fig. 3). Principal component analysis was performed and target maps

were constructed from cluster spectra for all analyzed combinations of principal components and cluster analyses. For each sample we tested combinations of 2–8 components and 2–10 clusters in order to optimize the fit by reducing the RMS error to <0.01 . For the overview of the microaggregate at a depth of 0–0.16 m with a resolution of 500 nm we determined that a combination of 6 components and 5 clusters yielded the greatest number of clusters with an RMS <0.01 . An analysis of a specific region within the microaggregate from 0–0.16 m at a scale of 50 nm revealed that a combination of 5 principal components and 8 clusters yielded the greatest number of clusters (the first 4) with RMS values <0.01 (Fig. 3). For the analysis of an entire microaggregate at a spatial resolution of 500 nm from a depth of 0.16–0.43 m (Fig. 4), 5 principal components combined with 5 clusters gave the best fit for the first 3 clusters (lowest RMS values, <0.01). The best fit for the spectra obtained at a resolution of 500 nm of a microaggregate from a depth of 0.43–0.67 m was found for 5 principal components with 4 clusters (Fig. 5).

Alkaline extract spectra obtained from each soil in the depth profile were searched for in the respective component/cluster combination representing the best fit for each map. No significant fits (criterion of RMS <0.01) were found for any of both soil alkaline extracts in their respective maps, and RMS values were 0.11 to 0.23 (Figs. 2–5).

4. Discussion

4.1. Functional group composition of alkaline extracts

The spectra of the alkaline extracts were characteristic for *Terra Preta de Indio* soils according to comparisons with previously published work using NEXAFS (Liang et al., 2006; Solomon et al., 2007). The major changes in functional group composition of the alkali-extracts with depth were an increase in the proportion of aromatic type C and O-alkyl type C. This may be explained by the greater proportion of BC as a fraction of total organic C with depth (Liang et al., 2013) since soils with greater BC concentrations will also show greater amounts of extractable BC (Madari et al., 2013) and greater aromaticity in alkaline extracts (Novotny et al., 2013). Together with a lack of a systematic difference between alkaline extracts, this result suggests that alkaline extracts do not provide useful information on SOM properties for the

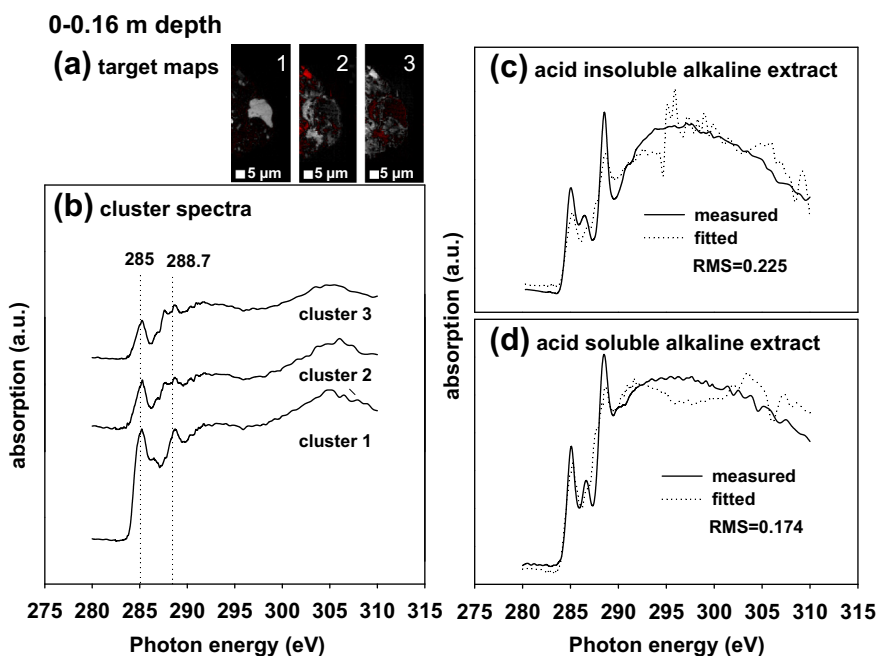


Fig. 2. Carbon 1s NEXAFS analysis of a microaggregate from an Amazonian Dark Earth at a depth of 0–0.16 m, using 500 nm step size; (a) target maps, (b) cluster spectra, (c) spectra and fit to acid-insoluble alkaline extract, and (d) spectra and fit to acid-soluble alkaline extract.

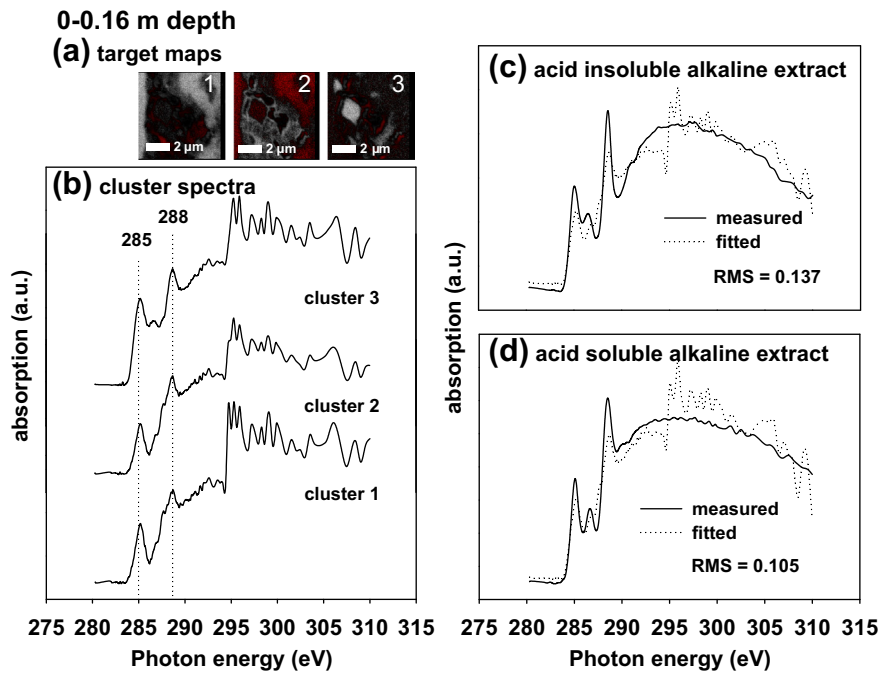


Fig. 3. Carbon 1s NEXAFS analysis of a portion of a microaggregate (from Fig. 2) from an Amazonian Dark Earth at a depth of 0–0.16 m, using 50 nm step size; (a) target maps, (b) cluster spectra, (c) spectra and fit to acid-insoluble alkaline extract, and (d) spectra and fit to acid-soluble alkaline extract.

studied BC-rich soils beyond trends discernable from bulk organic matter analyses.

4.2. Can spectral properties of alkaline extracts be found on a fine spatial scale?

The C functional group composition of the studied microaggregates using STXM resembles the results of earlier work on Amazonian Dark Earths (Lehmann et al., 2005; Liang et al., 2006). The poor fit of the NEXAFS spectra of alkaline extracts to microaggregates measured

using STXM suggests the absence of a distinct class of chemical compounds that can be isolated in this way, similarly observed by Lehmann et al. (2008) for BC-poor soils. These findings support a growing body of research which indicates that alkaline extraction does not isolate a distinct component class in soils or sediments that are often referred to as “humic substances”, but are instead the products of extraction. As already observed by Burdon (2001) even artifact formation is common in studies using alkaline extracts. Such assertions are not new (Kleber, 2010; Waksman, 1936). Evidence is growing to support the development of new language and methods by which to study soil

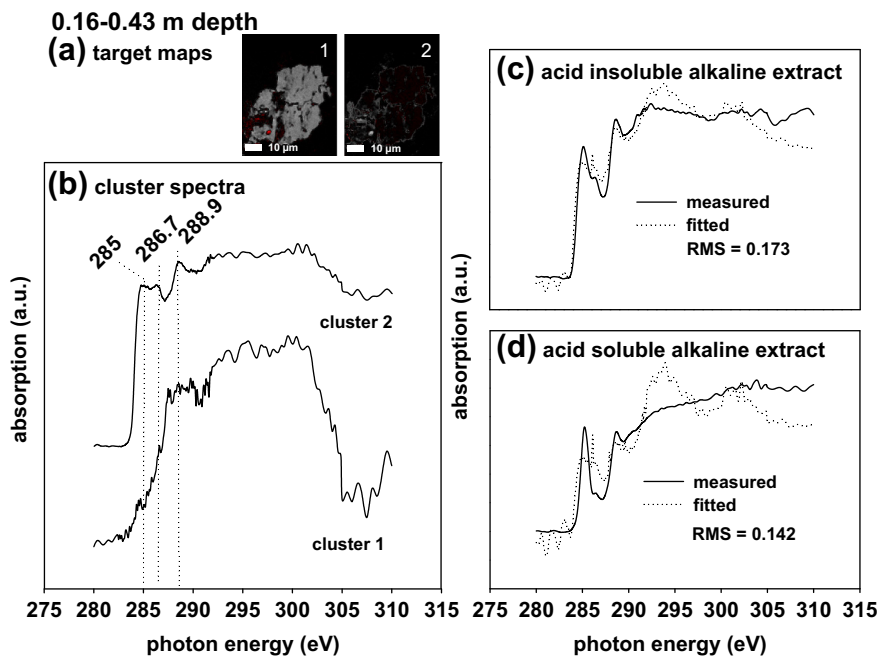


Fig. 4. Carbon 1s NEXAFS analysis of a microaggregate from an Amazonian Dark Earth at a depth of 0.16–0.43 m, using 500 nm step size; (a) target maps, (b) cluster spectra, (c) spectra and fit to acid-insoluble alkaline extract, and (d) spectra and fit to acid-soluble alkaline extract.

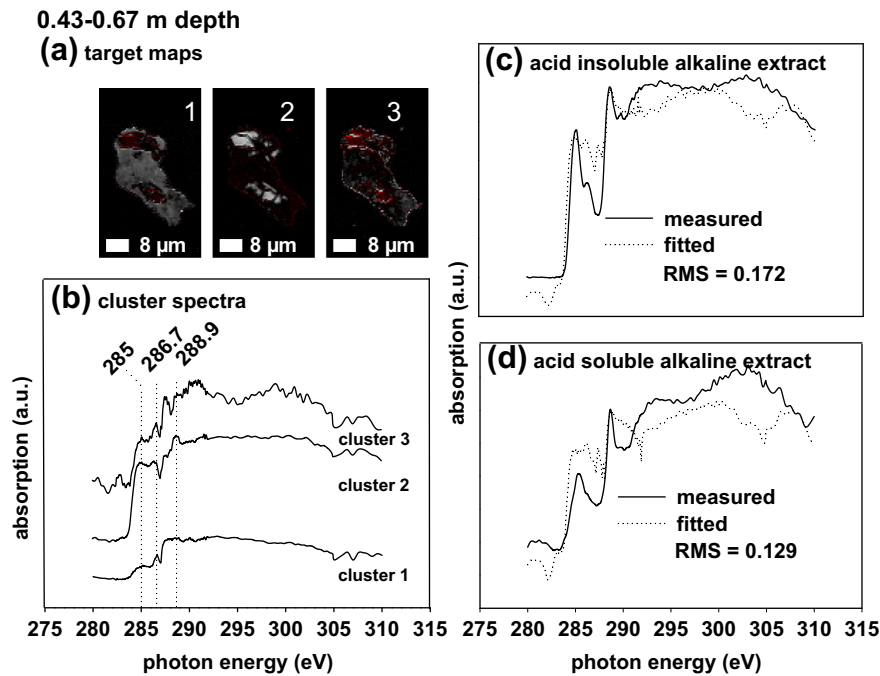


Fig. 5. Carbon 1s NEXAFS analysis of a microaggregate from an Amazonian Dark Earth at a depth of 0.43–0.67 m, using 500 nm step size; (a) target maps, (b) cluster spectra, (c) spectra and fit to acid-insoluble alkaline extract, and (d) spectra and fit to acid-soluble alkaline extract.

organic matter (Schmidt et al., 2011). According to our data, this conclusion also seems to hold with respect to “black humic substances” or “black humic acids”, which could not be identified at a fine spatial scale.

The fact that no soil organic matter components resembling the characteristics of soil alkaline extract spectra were directly observed at a fine spatial scale of less than 100 nm still leaves the question open for whether or not decomposition products of BC bear functional group characteristics of BC (Nishimura et al., 2006; Shindo et al., 2004). The lack of BC-type spectral characteristics in close proximity of micrometers to BC surfaces (Lehmann et al., 2008; Liang et al., 2013) may suggest that these instead more closely resemble other decomposition products rather than a distinct class characteristic of BC. Microbial metabolites would then undergo similar chemical decomposition processes regardless of whether they are generated from leaf litter or from BC, and would then undergo the same stabilization processes such as interactions with mineral surfaces and entrapment in pores inaccessible to decomposers (Schmidt et al., 2011).

5. Conclusions

We were not able to identify the spectral signature of alkaline extracts of BC-rich soils within the spatial maps of soil organic matter in microaggregates using NEXAFS and STXM at a spatial resolution of 50 nm. These results agree with more recent studies which question organic compounds extracted with alkaline solutions as an abundant and highly complex component of SOM. As recently suggested, alkaline extracts from environmental matrices such as soils and sediments should be increasingly scrutinized for their biogeochemical value. Future research should include stable isotope studies in combination with high-resolution mapping using Nano-SIMS and with compound-specific analyses that unequivocally demonstrate the nature and reactions of decomposition products of BC in soils.

Acknowledgments

This study was financially supported by grants from the NSF IGERT program (BCS-0215890), the NSF-Geobiology (EAR-0819689), USDA-AFRI (2008-35107-04511) and the Department of Crop and Soil

Sciences at Cornell University. Any opinions, findings and conclusions or recommendations expressed in this material are those of the authors and do not necessarily reflect the views of USDA or the National Science Foundation.

Appendix A. Supplementary data

Supplementary data to this article can be found online at <http://dx.doi.org/10.1016/j.geoderma.2014.07.011>.

References

- Ade, H., Hitchcock, A.P., 2008. NEXAFS microscopy and resonant scattering: composition and orientation probed in real and reciprocal space. *Polymer* 49, 643–675.
- Ade, H., Zhang, X., Cameron, S., Kirz, J., Williams, S., 1992. Chemical contrast in X-ray microscopy and spatially resolved XANES spectroscopy of organic specimen. *Science* 258, 972–975.
- Ascough, P.L., Bird, M.I., Francis, S.M., Lebl, T., 2011. Alkali extraction of archaeological and geological charcoal: evidence for diagenetic degradation and formation of humic acids. *J. Archaeol. Sci.* 38, 69–78.
- Baldock, J.A., Smernik, R.J., 2002. Chemical composition and bioavailability of thermally altered *Pinus resinosa* (Red Pine) wood. *Org. Geochem.* 33, 1093–1109.
- Boese, J., Osanna, A., Jacobsen, C., Kirz, J., 1997. Carbon edge XANES spectroscopy of amino acids and peptides. *J. Electron Spectrosc. Relat. Phenom.* 85, 9–15.
- Burdon, J., 2001. Are the traditional concepts of the structures of humic substances realistic? *Soil Sci.* 166, 752–769.
- Cheng, C., Lehmann, J., Engelhard, M.H., 2008. Natural oxidation of black carbon in soils: changes in molecular form and surface charge along a climosequence. *Geochim. Cosmochim. Acta* 72, 1598–1610.
- Cody, G.D., Ade, H., Wirick, S., Mitchell, G.D., Davis, A., 1998. Determination of chemical-structural changes in vitrinite accompanying luminescence alteration using C-NEXAFS analysis. *Org. Geochem.* 28, 441–455.
- Hedges, J.I., Eglinton, G., Hatcher, P.G., Kirchman, D.L., Arnosti, C., Derenne, S., Evershed, R.P., Kögel-Knabner, I., de Leeuw, J.W., Littke, R., Michaelis, W., Rullkötter, J., 2000. The molecularly-uncharacterized component of nonliving organic matter in natural environments. *Org. Geochem.* 31, 945–958.
- Heymann, K., Lehmann, J., Solomon, D., Schmidt, M.W.I., Regier, T., 2011. C 1s K-edge near edge X-ray absorption fine structure (NEXAFS) spectroscopy for characterizing functional group chemistry of black carbon. *Org. Geochem.* 42, 1055–1064.
- Hiradate, S., Nakadai, T., Shindo, H., Yoneyama, T., 2004. Carbon source of humic substances in some Japanese volcanic ash soils determined by carbon stable isotopic ratio, $\delta^{13}\text{C}$. *Geoderma* 119, 133–141.
- Hockaday, W.C., Grannas, A.M., Kim, S., Hatcher, P.G., 2006. Direct molecular evidence for the degradation and mobility of black carbon in soils from ultra high-resolution mass spectral analysis of dissolved organic matter from a fire-impacted forest soil. *Org. Geochem.* 37, 501–510.

- Jacobsen, C., Wirick, S., Flynn, G., Zimba, C., 2000. Soft X-ray spectroscopy from impage sequences with sub-100 nm spatial resolution. *J. Microsc.* 197, 173–184.
- Kelleher, B.P., Simpson, A.J., 2006. Humic substances in soils: are they really chemically distinct? *Environ. Sci. Technol.* 40, 4605–4611.
- Kinyangi, J., Solomon, D., Liang, B., Lerotic, M., Wirick, S., Lehmann, J., 2006. Nanoscale biogeochemical complexity of the organo-mineral assemblage in soil: application of STXM microscopy and C 1s-NEXAFS spectroscopy. *Soil Sci. Soc. Am. J.* 70, 1708–1718.
- Kleber, M., 2010. What is recalcitrant soil organic matter? *Environ. Chem.* 7, 320–332.
- Kleber, M., Johnson, M.G., 2010. Advances in understanding the molecular structure of soil organic matter; implications for interactions in the environment. *Adv. Soil Sci.* 106, 77–142.
- Kögel-Knabner, I., Zech, W., Hatcher, P.G., 1991. Chemical structural studies of forest soil humic acids: aromatic carbon fraction. *Soil Sci. Soc. Am. J.* 55, 241–247.
- Kumada, K., 1983. Carbonaceous materials as a possible source of soil humus. *Soil Sci. Plant Nutr.* 29, 383–386.
- Lehmann, J., Liang, B.Q., Solomon, D., Lerotic, M., Luizão, F., Kinyangi, J., Schäfer, T., Wirick, S., Jacobsen, C., 2005. Near-edge X-ray absorption fine structure (NEXAFS) spectroscopy for mapping nano-scale distribution of organic carbon forms in soil: application to black carbon particles. *Glob. Biogeochem. Cycles* 19, GB1013.
- Lehmann, J., Solomon, D., Kinyangi, J., Dathe, L., Wirick, S., Jacobsen, C., 2008. Spatial complexity of soil organic matter forms at nanometer scales. *Nat. Geosci.* 1, 238–242.
- Lehmann, J., Brandes, J., Fleckenstein, H., Jacobsen, C., Solomon, D., Thieme, J., 2009. Synchrotron-based near-edge X-ray spectroscopy of natural organic matter in soils and sediments. In: Senesi, N., Xing, B., Huang, P.M. (Eds.), *Biophysical–Chemical Processes Involving Natural Nonliving Organic Matter in Environmental Systems*. IUPAC Series on Biophysico-Chemical Processes in Environmental Systems. Wiley, New Jersey, pp. 729–781.
- Liang, B., Lehmann, J., Solomon, D., Kinyangi, J., Grossman, J., O'Neill, B., Skjemstad, J.O., Thies, J., Luizão, F.J., Petersen, J., Neves, E.G., 2006. Black carbon increases cation exchange capacity in soils. *Soil Sci. Soc. Am. J.* 70, 1719–1730.
- Liang, B., Lehmann, J., Solomon, D., Sohi, S., Thies, J.E., Skjemstad, J.O., Luizão, F.J., Engelhard, M.H., Neves, E.G., Wirick, S., 2008. Stability of biomass-derived black carbon in soils. *Geochim. Cosmochim. Acta* 72, 6069–6078.
- Liang, B., Wang, C.H., Solomon, D., Kinyangi, J., Luizão, F.J., Wirick, S., Skjemstad, J.O., Lehmann, J., 2013. Oxidation is key for black carbon surface functionality and nutrient retention in Amazon Anthrosols. *Br. J. Environ. Clim. Chang.* 3, 9–23.
- Madari, B.E., Lime, L.B., Silva, M.A.S., Novotny, E.H., Alcantara, F.A., Carvalho, M.T.M., Petter, F.A., 2013. Carbon distribution in humic substance fractions extracted from soils treated with charcoal (biochar). In: Xu, J., Wu, J., He, Y. (Eds.), *Functions of Natural Organic Matter in Changing Environment*. Springer, Dordrecht, pp. 1003–1006.
- Masiello, C.A., Druffel, E.R.M., 1998. Black carbon in deep-sea sediments. *Science* 280, 1911–1913.
- Nishimura, S., Tani, M., Fujitake, N., Shindo, H., 2006. Relationship between distribution of charred plant residues and humus composition in chernozemic soils. *Pedologist* 53, 86–93.
- Novotny, E.H., Aucaise, R., Lima, L.B., Madari, B.E., 2013. Characterisation of humic substances extracted from soil treated with charcoal (biochar). In: Xu, J., Wu, J., He, Y. (Eds.), *Functions of Natural Organic Matter in Changing Environment*. Springer, Dordrecht, pp. 971–974.
- Ravel, B., Newville, M., 2005. Athena, artemis, hephaestus. *J. Synchrotron Radiat.* 12, 537–541.
- Schäfer, T., Michel, P., Claret, F., Beetz, T., Wirick, S., Jacobsen, C., 2009. Radiation sensitivity of natural organic matter: clay mineral association effects in the Callovo–Oxfordian argillite. *J. Electron Spectrosc. Relat. Phenom.* 170, 49–56.
- Scheinost, A.C., Kretschmar, R., Christl, I., Jacobsen, C., 2001. Carbon group chemistry of humic and fulvic acid: a comparison of C 1s NEXAFS and ¹³C NMR spectroscopies. In: Ghabbour, E.A., Davies, G. (Eds.), *Humic Substances: Structures, Models and Functions*. Royal Society of Chemistry, Cambridge, UK, pp. 39–47.
- Schmidt, M.W.L., Torn, M.S., Abiven, S., Dittmar, T., Guggenberger, G., Janssens, I.A., Kleber, M., Kögel-Knabner, I., Lehmann, J., Manning, D.A.C., Nannipieri, P., Rasse, D.P., Weiner, S., Trumbore, S.E., 2011. Persistence of soil organic matter as an ecosystem property. *Nature* 478, 49–56.
- Schulten, H.R., Schnitzer, M., 1993. A state of the art of the structural concept for humic substances. *Naturwissenschaften* 28, 311–312.
- Schuur, E.A.G., Abbott, B.W., Bowden, W.B., Brovkin, V., Camill, P., Canadell, J.G., Chanton, J.P., Chapin III, F.S., Christensen, T.R., Ciais, P., Crosby, B.T., Czimczik, C.I., Grosse, G., Harden, J., Hayes, D.J., Hugelius, G., Jastrow, J.D., Jones, J.B., Kleinen, T., Koven, C.D., Krinner, G., Kuhry, P., Lawrence, D.M., McGuire, A.D., Natali, S.M., O'Donnell, J.A., Ping, C.L., Riley, W.J., Rinke, A., Romanovsky, V.E., Sannel, A.B.K., Schädel, C., Schaefer, K., Sky, J., Subin, Z.M., Tamocai, C., Turetsky, M.R., Waldrop, M.P., Walter Anthony, K.M., Wickland, K.P., Wilson, C.J., Zimov, S.A., 2013. Expert assessment of vulnerability of permafrost carbon to climate change. *Clim. Chang.* 119, 359–374.
- Sham, T.K., Yang, B.X., Kirz, J., Tse, J.S., 1989. K-edge near-edge x-ray-absorption fine structure of oxygen- and carbon-containing molecules in the gas phase. *Phys. Rev. A* 40, 652–669.
- Shindo, H., Honna, T., Yamamoto, S., Honma, H., 2004. Contribution of charred plant fragments to soil organic carbon in Japanese volcanic ash soils containing black humic acids. *Org. Geochem.* 35, 235–241.
- Shindo, H., Matsui, Y., Higashi, T., 1986a. A possible source of humic acids in volcanic ash soils in Japan – charred residue of *Miscanthus sinensis*. *Soil Sci.* 141, 84–87.
- Shindo, H., Higashi, T., Matsui, Y., 1986b. Comparison of humic acids from charred residues of Susuki (*Eulalia*, *Miscanthus sinensis* A.) and from the A horizons of volcanic ash soils. *Soil Sci. Plant Nutr.* 32, 579–586.
- Shindo, H., Matsui, Y., Higashi, T., 1986c. Humus composition of charred plant residues. *Soil Sci. Plant Nutr.* 32, 475–478.
- Shindo, H., Miho, Y., Yamamoto, A., Honma, H., Syuntaro, H., 2005. $\delta^{13}\text{C}$ values of organic constituents and possible source of humic substances in Japanese volcanic ash soils. *Soil Sci.* 170, 175–182.
- Solomon, D., Lehmann, J., Thies, J., Schäfer, T., Liang, B., Kinyangi, J., Neves, E., Petersen, J., Luizão, F., Skjemstad, J.O., 2007. Molecular signature and sources of biochemical recalcitrance of organic C in Amazonian Dark Earths. *Geochim. Cosmochim. Acta* 71, 2285–2298.
- Solomon, D., Lehmann, J., Kinyangi, J., Liang, B.Q., Heymann, K., Dathe, L., Hanley, K., Wirick, S., Jacobsen, C., 2009. Carbon (1s) NEXAFS spectroscopy of biogeochemically relevant reference organic compounds. *Soil Sci. Soc. Am. J.* 73, 1817–1830.
- Stevenson, F.J., 1994. *Humus Chemistry: Genesis, Composition Reactions*, 2nd ed. John Wiley and Sons, Inc., New York.
- Sutton, R., Sposito, G., 2005. Molecular structure in soil humic substances: the new view. *Environ. Sci. Technol.* 39, 9009–9015.
- Swift, R.S., 1996. Organic matter characterization. In: Sparks, D.L., Bartels, J.M., Bigham, J.M. (Eds.), *Methods of Soil Analysis. Part 3. Agron. Monogr.*, 5. ASA, SSSA, Madison, Wisconsin, pp. 1018–1020.
- Waksman, S.A., 1936. *Humus*. Bailliére, Tindall and Cox, London.
- Winn, B., Ade, H., Buckley, C., Feser, M., Howells, M., Hulbert, S., Jacobsen, C., Kaznacheyev, K., Kirz, J., Osanna, A., Maser, J., McNulty, I., Miao, J., Oversluisen, T., Spector, S., Sullivan, B., Wang, S., Wirick, S., Zhang, H., 2000. Illumination for coherent soft x-ray applications: the new X1A beamline at the NSLS. *J. Synchrotron Radiat.* 7, 395–404.